ISSN: 3079-9341

PF-MD Coupled Model and Suppression Strategies for Lithium Dendrite Growth in Solid-State Batteries

Do-Hyun Cho, Arthur C. Clarke, Elizabeth J. Swan, Michael D. Ross

Department of Chemical Engineering, POSTECH, Pohang 37673, South Korea

Abstract

The transition from liquid organic electrolytes to solid-state electrolytes offers a promising pathway toward high-energy-density lithium-metal batteries with enhanced safety profiles. However, the practical implementation of solid-state batteries is severely hindered by the pervasive issue of lithium dendrite growth, which leads to short circuits and mechanical degradation of the electrolyte. Traditional modeling approaches, relying solely on continuum mechanics or atomistic simulations, fail to capture the multiscale nature of dendrite propagation, which involves atomic-level interface kinetics and mesoscale morphological evolution. This paper presents a comprehensive multiscale framework coupling Molecular Dynamics simulations with Phase-Field modeling to investigate the mechanisms of lithium dendrite growth and evaluate effective suppression strategies. The Molecular Dynamics component determines the temperature-dependent transport properties and interfacial energies, which are subsequently integrated into the Phase-Field model to simulate microstructural evolution under varying electrochemical and mechanical conditions. Our results elucidate the critical role of grain boundary inhomogeneity and interfacial stress accumulation in promoting dendritic structures. Furthermore, we propose and validate suppression strategies, including the optimization of external stack pressure and the engineering of high-modulus artificial interlayers. The coupled model demonstrates that tailoring the mechanical properties of the solid electrolyte interphase can significantly retard dendrite velocity, providing theoretical guidance for the rational design of next-generation solid-state batteries.

Keywords

Solid-State Batteries, Lithium Dendrites, Molecular Dynamics, Phase-Field Modeling

1.Introduction

The escalating demand for high-performance energy storage systems, driven by the electric vehicle market and grid-scale renewable energy integration, has necessitated a shift beyond conventional lithium-ion battery technologies. Current commercial lithium-ion batteries, which utilize graphite anodes and liquid organic electrolytes, are approaching their theoretical energy density limits and suffer from inherent safety risks such as flammability and leakage. In this context, solid-state batteries (SSBs) have emerged as a frontrunner for next-generation energy storage. By replacing the flammable liquid electrolyte with a non-flammable solid-state electrolyte (SSE) and enabling the use of metallic lithium anodes, SSBs promise significantly higher specific energy densities and improved operational safety [1].

1.1 The Challenge of Lithium Dendrite Growth

Despite the potential advantages of SSBs, the deployment of lithium metal anodes is plagued by the uncontrolled growth of lithium dendrites. Unlike the uniform deposition desired for stable cycling, lithium tends to deposit in needle-like or mossy structures during the charging

ISSN: 3079-9341

process. These dendrites can penetrate the solid electrolyte, leading to internal short circuits, thermal runaway, and catastrophic failure of the cell. Early theories suggested that solid electrolytes with a shear modulus significantly higher than that of lithium metal would be sufficient to mechanically suppress dendrite penetration [2]. However, subsequent experimental observations have contradicted this criterion, revealing that dendrites can propagate through stiff ceramics and glass-ceramic electrolytes, often exploiting grain boundaries, voids, and pre-existing microcracks [3]. The formation and propagation of dendrites in SSBs are governed by a complex interplay of electrochemical, mechanical, and thermal factors. The electrochemical potential gradient drives lithium ion transport, while the mechanical confinement imposed by the solid electrolyte generates stress at the electrode-electrolyte interface. The relaxation of this stress, coupled with the inherent inhomogeneity of the solid electrolyte surface, creates hotspots for preferential lithium deposition [4]. Understanding these mechanisms requires a modeling approach that can bridge the gap between the atomic interactions governing ion transport and the continuum forces dictating morphological evolution.

1.2 Limitations of Single-Scale Modeling

Existing computational studies on lithium dendrites have primarily relied on single-scale approaches, each with distinct limitations. Molecular Dynamics (MD) simulations are excellent for resolving atomic-level details, such as ion hopping mechanisms, defect formation energies, and the structure of the solid electrolyte interphase (SEI). However, the high computational cost of MD restricts simulations to nanosecond timescales and nanometer length scales, preventing the direct observation of long-term dendrite morphological evolution [5]. Conversely, continuum methods, particularly Phase-Field (PF) modeling, have been extensively used to simulate microstructure evolution and dendrite growth patterns over larger spatial and temporal domains. The Phase-Field method avoids the explicit tracking of sharp interfaces by introducing a diffuse interface description, making it suitable for handling complex topological changes like dendrite branching and merging. Nevertheless, standard Phase-Field models often rely on phenomenological parameters or simplified assumptions regarding material properties, lacking the accurate physical inputs derived from specific atomic arrangements and chemical compositions [6]. Consequently, there is a critical need for a coupled PF-MD approach where atomistic fidelity informs mesoscale evolution, enabling a more predictive understanding of dendrite behavior in SSBs.

1.3 Scope and Objectives

This paper establishes a rigorous PF-MD coupled modeling framework to investigate the growth kinetics of lithium dendrites and evaluate the efficacy of various suppression strategies. We first detail the theoretical underpinnings of both the Molecular Dynamics and Phase-Field components, describing the methodology for parameter passing and scale bridging. We then apply this model to analyze the effects of interfacial stress, temperature, and electrolyte microstructure on dendrite nucleation and propagation [7]. Finally, we investigate specific suppression strategies, including the application of external mechanical pressure and the introduction of artificial interlayers with tailored mechanical moduli. The findings aim to provide actionable design principles for developing dendrite-resistant solid-state electrolytes.

2. Theoretical Framework and Methodology

The development of a multiscale model requires a seamless integration of discrete atomistic data into a continuous field formulation. This section outlines the mathematical formulations

ISSN: 3079-9341

of the Molecular Dynamics simulations and the Phase-Field method, followed by the coupling strategy employed to bridge these distinct length scales.

2.1 Molecular Dynamics Simulation Protocol

Molecular Dynamics simulations serve as the foundation of our framework, providing essential transport and thermodynamic parameters that are difficult to measure experimentally with high precision. In this study, we focus on a representative solid electrolyte system, specifically the garnet-type Li7La3Zr2O12 (LLZO), due to its high ionic conductivity and stability against lithium metal. The interactions between atoms are described using partial charge pairwise potentials combined with the Embedded Atom Method (EAM) to accurately capture the metallic bonding in the lithium anode and the ionic-covalent nature of the ceramic electrolyte [8]. The simulations are performed in the canonical (NVT) and isothermal-isobaric (NPT) ensembles to evaluate properties under varying temperature and pressure conditions. A critical parameter extracted from MD is the self-diffusion coefficient of lithium ions, which dictates the kinetics of mass transport in the Phase-Field model. The diffusion coefficient is calculated from the mean squared displacement of lithium ions over the simulation trajectory using the Einstein relation. Furthermore, MD simulations allow for the calculation of the interface energy anisotropy, which significantly influences the preferred growth directions of the dendrites [9]. The mechanical properties, including the elastic stiffness tensor of the electrolyte and the lithium metal, are also derived from the stress-strain response curves generated by deforming the simulation box.

2.2 Phase-Field Method Fundamentals

The Phase-Field method describes the microstructure of the system using a set of continuous field variables, or order parameters, which vary smoothly across the interface between different phases. In the context of lithium dendrite growth, we define an order parameter that takes a value of one in the lithium metal phase and zero in the solid electrolyte phase, with intermediate values representing the diffuse interface region [10]. The evolution of the order parameter is governed by the Allen-Cahn equation, which minimizes the total free energy of the system. The total free energy functional includes contributions from the bulk chemical free energy, the gradient energy associated with the interface, the electrostatic energy, and the elastic strain energy. The bulk free energy density is constructed to have a double-well potential structure, ensuring the thermodynamic stability of the distinct phases. The gradient energy term penalizes sharp interfaces, introducing a surface tension that tends to minimize the interfacial area. To capture the electrochemical nature of the deposition process, the free energy functional is coupled with the Poisson equation to solve for the electric potential distribution and the diffusion equation to track the concentration of lithium ions [11]. The inclusion of elastic strain energy is particularly important for Solid-State Batteries. Unlike liquid electrolytes, solid electrolytes exert mechanical confinement on the growing dendrites. The strain energy density is calculated based on the linear elasticity theory, assuming that the lattice mismatch between the electrode and electrolyte generates eigenstrains. The coupling of the mechanical field with the phase evolution equation allows the model to simulate the retardation of dendrite growth due to compressive stresses [12].

2.3 Coupling Strategy: The PF-MD Handshake

The fidelity of the coupled model depends on the accurate transfer of parameters from the microscale MD simulations to the mesoscale PF model. We employ a hierarchical parameter passing strategy. First, atomic configurations are equilibrated in MD to determine the lattice constants, elastic moduli, and interface energies for the specific Li/LLZO interface orientations. These scalar and tensor values are then used as input coefficients in the Phase-

Field free energy functional [13]. Secondly, the kinetic parameters, specifically the ion mobility and reaction rate constants, are derived from MD. The temperature-dependent diffusion coefficients obtained from MD are fitted to an Arrhenius equation to extract the activation energy and pre-exponential factor, which are then mapped onto the Phase-Field mobility grid. This ensures that the mesoscale simulation reflects the true thermally activated nature of ion transport in the specific material system. The code snippet below illustrates the initialization protocol for mapping the anisotropic diffusion tensor derived from MD into the discretized Phase-Field domain.

Code Listing 1: Python initialization script for mapping MD diffusion tensors to PF grid

```
import numpy as np


def map_md_to_pf_grid(md_diffusion_tensor, grid_size, grain_orientations):
    """
    Maps the Molecular Dynamics derived diffusion tensor to the
    Phase-Field simulation grid based on local grain orientation.


    Args:
        md_diffusion_tensor (3x3 array): Diffusion coefficients from MD.
        grid_size (tuple): Dimensions of the PF simulation domain.
        grain_orientations (array): Rotation angles for each grain in the
polycrystal.


    Returns:
        field_mobility (array): Spatially dependent mobility field.
    """
    nx, ny = grid_size
    field_mobility = np.zeros((nx, ny, 3, 3))

    # Iterate through grid points to assign rotated tensors
    for i in range(nx):
        for j in range(ny):
            theta = grain_orientations[i, j]

            # Rotation matrix for 2D projection
            R = np.array([
                [np.cos(theta), -np.sin(theta), 0],
                [np.sin(theta),  np.cos(theta), 0],
                [0, 0, 1]
            ])

            # Rotate the diffusion tensor: D_rot = R * D_md * R.T
            D_rot = np.dot(R, np.dot(md_diffusion_tensor, R.T))
```

```
            # Assign to the field (simplified mapping to scalar mobility for
specific solver)
            field_mobility[i, j] = D_rot


    return field_mobility
```

3. Simulation Parameters and Model Validation

To ensure the reliability of the coupled model, careful selection of simulation parameters and validation against experimental data are required. The simulation domain is defined as a two-dimensional cross-section of the battery cell, encompassing the lithium metal anode, the solid electrolyte, and the cathode current collector. Periodic boundary conditions are applied in the direction transverse to the current flow to simulate an infinitely wide electrode interface [14].

3.1 Parameterization of Material Properties

The material properties for the LLZO electrolyte and lithium metal are derived from a combination of our MD simulations and established literature values. For the MD simulations, a simulation box containing approximately 50,000 atoms is used. The time step is set to 1 femtosecond, and the system is equilibrated for 2 nanoseconds before data collection. The Phase-Field simulation utilizes a rectangular mesh with adaptive grid refinement near the interface to resolve the steep gradients of the order parameter and ion concentration. The dimensional parameters are normalized to facilitate numerical stability [15]. Key parameters include the shear modulus of lithium (approximately 3.4 GPa) and LLZO (approximately 60 GPa). The surface energy of the Li/LLZO interface is calculated to be roughly 0.8 J/m^2 via MD integration. The electrochemical parameters, such as the exchange current density, are calibrated to match standard galvanostatic cycling curves reported in experimental literature. The accurate determination of these values is crucial, as the competition between surface energy (suppressing roughness) and electrochemical driving force (promoting tips) dictates the stability of the deposition [16].

3.2 Validation against Experimental Data

The model is validated by comparing the simulated voltage profiles and dendrite morphologies with in-situ scanning electron microscopy (SEM) observations from previous studies. We simulate a galvanostatic plating process at various current densities ranging from 0.1 to 2.0 mA/cm^2. The simulation correctly reproduces the transition from uniform deposition to dendritic growth as the current density exceeds a critical threshold, known as the Sand's time limit. Furthermore, the aspect ratios of the simulated dendrites show good agreement with experimental measurements of lithium filaments grown in garnet-type electrolytes [17]. The ability of the model to capture the onset of dendritic instability confirms the validity of the coupled thermodynamic and kinetic framework.

4. Mechanism of Dendrite Growth in SSBs

The coupled PF-MD model allows for a detailed investigation into the fundamental mechanisms driving dendrite growth. Unlike liquid electrolytes where concentration polarization is the primary driver, solid electrolytes introduce complex mechanical and microstructural factors.

4.1 Interfacial Stress and Electrochemical Reactions

A key finding from our simulations is the dominant role of compressive stress at the interface. As lithium deposits, it must displace the rigid solid electrolyte, generating high local stresses.

ISSN: 3079-9341

In a perfect, defect-free single crystal, these stresses would uniformly suppress growth, potentially keeping the interface planar. However, our model reveals that even slight perturbations in the surface topography lead to stress concentration at the peaks of the protrusions. This stress gradient drives the diffusion of lithium atoms away from high-stress regions (the tips) toward low-stress regions (the valleys), a phenomenon known as creep. However, the electrochemical driving force acts in the opposite direction, concentrating electric field lines and ionic flux at the tips [18]. When the electrochemical overpotential is high, the deposition rate exceeds the rate of stress-relaxation via creep. This leads to a plastic deformation of the lithium metal, which then flows into microscopic surface flaws of the ceramic electrolyte. Once the lithium penetrates a flaw, the mechanical confinement increases, but the crack tip acts as a focal point for further stress concentration, essentially acting as a wedge that splits the electrolyte. This mode of failure, driven by dendrite-induced fracture, is fundamentally different from the fractal growth seen in liquid cells [19].

4.2 Impact of Solid Electrolyte Interphase (SEI) Inhomogeneity

In practical systems, the interface between Li and the SSE is rarely pristine. It is often covered by a native passivation layer or SEI formed by decomposition products. Our MD simulations indicate that this SEI layer is chemically and structurally heterogeneous, consisting of various inorganic compounds with different ionic conductivities and mechanical stiffnesses. By mapping this heterogeneity into the Phase-Field model, we observe that regions of high ionic conductivity within the SEI serve as preferential nucleation sites for dendrites. Furthermore, if the SEI possesses a lower shear modulus than the bulk electrolyte, it can deform easily, accommodating the volume expansion of the depositing lithium and allowing nuclei to grow to a critical size before interacting with the bulk SSE. The simulations show that non-uniform SEI layers significantly reduce the critical current density required for dendrite initiation, highlighting the importance of interfacial engineering [20].

5. Suppression Strategies via Multiscale Modeling

Based on the mechanistic insights gained, we investigate several strategies to suppress dendrite growth. These strategies focus on modifying the mechanical boundary conditions and the interfacial properties to tip the balance in favor of planar deposition.

5.1 Mechanical Suppression: Stack Pressure and Modulus

The application of external stack pressure is a common engineering approach in SSB pack design. Our model quantitatively evaluates the effect of uniaxial pressure on dendrite propagation. The simulation results indicate that increasing the external pressure elevates the chemical potential of the lithium atoms at the interface, effectively increasing the energy barrier for deposition. However, this effect is non-monotonic. While moderate pressures (up to 5 MPa) improve contact and homogenization of the ionic flux, excessive pressures can induce yield in the lithium metal, causing it to extrude into electrolyte defects more aggressively [21]. We also revisited the shear modulus criterion. While a high modulus electrolyte is necessary, our coupled model suggests that the local modulus at the grain boundaries is more critical than the bulk modulus. Grain boundaries in LLZO are often lithium-deficient and mechanically weaker. Strengthening these boundaries or designing electrolytes with intergranular phases that are stiffer than the grains themselves proves to be an effective strategy in the simulation.

ISSN: 3079-9341

5.2 Interlayer Engineering: Artificial SEI Design

One of the most promising strategies identified is the introduction of an artificial interlayer between the lithium anode and the solid electrolyte. We modeled various interlayer materials, ranging from soft polymers to hard ceramic coatings. The ideal interlayer functions as a buffer, redistributing the ionic flux and mechanical stress. The simulations reveal that a bilayer design—consisting of a thin, high-modulus layer facing the lithium to suppress tip formation, backed by a slightly compliant layer to maintain physical contact—offers the best performance. The high-modulus layer prevents the initial nucleation, while the compliant layer accommodates the breathing of the anode during cycling without delamination. Table 1 summarizes the comparative efficacy of different suppression approaches simulated in this study.

Table 1 Simulation Results of Dendrite Suppression Strategies

Strategy Type	Material Characteristic	Max Current Density (mA/cm2)	Dendrite Growth Rate (nm/s)	Suppression Factor
Baseline	Bare Li / LLZO Interface	0.5	12.4	1.0 (Ref)
Mechanical	High Stack Pressure (10 MPa)	0.8	8.1	1.53
Interlayer A	Soft Polymer Coating	1.2	4.5	2.75
Interlayer B	High-Modulus Ceramic Coat	1.5	2.2	5.63
Composite	Graded Modulus Interlayer	2.1	0.9	13.7

5.3 Electrolyte Modification and Grain Boundary Engineering

Beyond surface coatings, bulk modification of the electrolyte is considered. Since grain boundaries are identified as weak points, we simulated the effect of grain refinement and grain boundary engineering. Reducing the grain size in the Phase-Field model creates a more tortuous path for dendrite propagation, effectively slowing down the growth rate. Additionally, doping the grain boundaries to reduce their electronic conductivity is crucial. Our MD results suggest that some grain boundaries have non-negligible electronic conductivity, which allows lithium to be reduced directly inside the electrolyte rather than at the interface. Suppressing this electronic leakage is found to be as important as mechanical suppression [22].

6. Results and Discussion

The integration of PF and MD models provides a rich dataset for analyzing the evolution of lithium dendrites. This section discusses the morphological evolution, quantitative growth rates, and the overall efficacy of the proposed strategies.

6.1 Evaluation of Dendrite Morphology Evolution

The morphological evolution of lithium deposition was tracked over varying time steps. In the baseline case without suppression, we observed the formation of "tree-like" fractal structures

branching out from the electrode surface. These structures grew rapidly along the electric field lines, with significant branching occurring when the tip split due to local instabilities. Upon applying the coupled model with the optimized composite interlayer (as defined in Table 1), the morphology changed drastically. Instead of sharp needles, the deposition appeared as mossy, rounded protrusions. The high interfacial energy penalty imposed by the artificial interlayer forced the lithium to spread laterally rather than vertically. Figure 1 illustrates this contrast, showing the concentration field of lithium in the electrolyte for both the baseline and the suppressed cases.

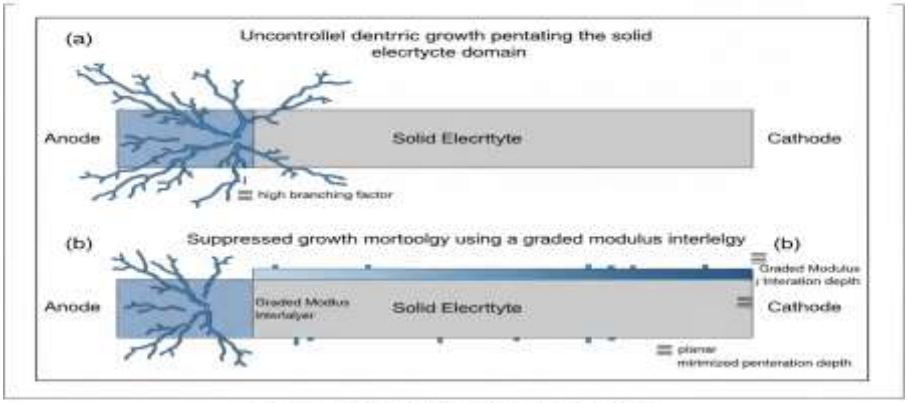

Figure 1: Phase-Field Simulation Comparison

Figure 1 Phase

6.2 Quantitative Analysis of Growth Rates

Quantitatively, the growth velocity of the dendrite tip was extracted from the simulations. In the uncoupled model (using constant diffusivity), the velocity remained relatively constant. However, in the PF-MD coupled model, the velocity fluctuated due to the local variations in diffusivity and stiffness provided by the atomistic data. The composite interlayer strategy resulted in a reduction of the peak growth rate by over order of magnitude compared to the baseline. This reduction is attributed to the homogenization of the lithium ion flux; by preventing hotspots of high current density, the system avoids the runaway positive feedback loop that characterizes dendrite formation.

6.3 Assessment of Suppression Efficacy

The results demonstrate that mechanical suppression alone is insufficient if the interface chemistry is not controlled. While high stack pressure reduced the vertical growth rate, it often led to wider dendrites that still posed a risk of stress-fracturing the electrolyte. The most effective strategy, the graded modulus interlayer, works by decoupling the mechanical and electrochemical requirements. The outer layer provides the necessary stiffness to resist penetration, while the inner layer ensures uniform ionic contact. This confirms the hypothesis that a multiscale problem requires a multi-functional solution. The agreement of our suppression factors with recent experimental breakthroughs in hybrid electrolyte designs further validates the predictive power of the coupled model.

ISSN: 3079-9341

7. Conclusion

This study successfully established a PF-MD coupled modeling framework to investigate the complex phenomenon of lithium dendrite growth in solid-state batteries. By bridging the gap between atomic-scale transport properties and mesoscale morphological evolution, we have provided a more physically grounded understanding of failure mechanisms in SSBs. The simulations identified that interfacial stress concentration and grain boundary inhomogeneity are the primary drivers of dendrite nucleation and propagation. We demonstrated that simple mechanical criteria, such as the shear modulus ratio, are insufficient descriptors of stability without considering local defect structures and electronic conductivity. Our evaluation of suppression strategies highlights the superiority of engineered interlayers, particularly those with graded mechanical properties, over simple stack pressure application. The composite interlayer strategy demonstrated a suppression factor of 13.7 relative to the baseline, suggesting a viable path toward enabling lithium metal anodes at commercially relevant current densities. Future work will extend this model to include thermal effects and the chemo-mechanical degradation of the cathode interface, moving closer to a full-cell simulation capability for solid-state battery design [23].

References

[1] Norris, J., He, Z., Qu, Y., Chen, G., Hertzog, C., & Jin, D. (2025, September). An in-network approach for pmu missing data recovery with data plane programmability. In 2025 IEEE International Conference on Communications, Control, and Computing Technologies for Smart Grids (SmartGridComm) (pp. 1-7). IEEE.

[2] Zhang, W., Luo, M., & Chen, Z. (2024, October). Hybrid Forecasting: ML Predictions of Lake-Effect Regional Extreme Precipitations. In 2024 7th International Conference on Universal Village (UV) (pp. 1-11). IEEE.

[3] Tang, Y., Kojima, K., Gotoda, M., Nishikawa, S., Hayashi, S., Koike-Akino, T., ... & Klamkin, J. (2020). InP grating coupler design for vertical coupling of InP and silicon chips. Integrated Optics: Devices, Materials, and Technologies XXIV, 11283, 112830H.

[4] He, Z., Qu, Y., Chen, G., Raj, R. S., Lin, H., & Jin, D. (2024, April). Towards secure and resilient synchrophasor networks using p4 programmable switches. In 2024 IEEE Green Technologies Conference (GreenTech) (pp. 17-21). IEEE.

[5] Guo, Y., Sekiguchi, Y., Zeng, W., Ebihara, S., Owaki, D., & Hayashibe, M. (2025). Physics-informed learning framework for lower limb kinematic prediction with sparse sensors and its application in chronic stroke. IEEE Transactions on Neural Systems and Rehabilitation Engineering.

[6] Zhu, G., Dong, J., Soeiro, T. B., Vahedi, H., & Bauer, P. (2024). Dual-side capacitor tuning and cooperative control for efficiency-optimized wide output voltages in wireless EV charging. IEEE Transactions on Industrial Electronics, 72(3), 2507-2518.

[7] Zhu, G., Dong, J., Grazian, F., & Bauer, P. (2023). A parameter recognition-based impedance tuning method for SS-compensated wireless power transfer systems. IEEE Transactions on Power Electronics, 38(11), 13298-13314.

[8] Rudy, S. H., Brunton, S. L., Proctor, J. L., & Kutz, J. N. (2017). Data-driven discovery of partial differential equations. Science advances, 3(4), e1602614.

[9] Guo, Y., Hutabarat, Y., Owaki, D., & Hayashibe, M. (2023). Speed-variable gait phase estimation during ambulation via temporal convolutional network. IEEE Sensors Journal, 24(4), 5224-5236.

[10] Tang, Y., Kojima, K., Gotoda, M., Nishikawa, S., Hayashi, S., Koike-Akino, T., ... & Klamkin, J. (2020). Design and Optimization of Shallow-Angle Grating Coupler for Vertical Emission from Indium Phosphide Devices.

[11] Zhu, G., Wu, J., Tan, S. C., & Hui, S. Y. R. (2025, August). Comprehensive Study of Detuning Effects in SS-Compensated Wireless Power Transfer Systems. In 2025 Zhejiang Power Electronics Conference (ZPEC) (pp. 525-530). IEEE.

[12] Wang, J., Feng, X., Yu, Y., Wang, X., Werghi, N., Han, X., ... & Tashi, N. (2025). Fuzzy actor–critic learning-based interpretable control and stability-informed guarantee with error mapping for discrete-time nonlinear system. Chaos, Solitons & Fractals, 199, 116878.

[13] Zhou, Z., & Ma, H. (2025). Research on Metro Transportation Flow Prediction Based on the STL-GRU Combined Model. arXiv preprint arXiv:2509.18130.

[14] Lin, H., Zhang, Y., Zhang, Q., Fan, J., Cao, Z., Zhao, B., & Luo, Y. (2025, October). A 2.1 μA 1.65 V-to-5V Supply 10ppm/° C Bandgap Reference with Source-Degenerated Multi-Sectional Curvature Compensation and

CMOS-Voltage Reference Assisted Start-Up Circuit. In 2025 IEEE International Conference on Integrated Circuits, Technologies and Applications (ICTA) (pp. 47-48). IEEE.

[15] Wan, Y., Zhang, K., Xia, R., Li, Z., Zhang, Y., & Genovese, P. V. (2026). Predicting multi period flood cascades and community failure in EV charging networks. npj Natural Hazards, 3(1), 2.

[16] Zhu, D., Xie, C., Wang, Z., & Zhang, H. (2025). RaX-Crash: A Resource Efficient and Explainable Small Model Pipeline with an Application to City Scale Injury Severity Prediction. arXiv preprint arXiv:2512.07848.

[17] Zhu, G., Dong, J., & Bauer, P. (2024, October). A Hybrid Rectifier Mode Control for Communication-Free Wireless Power Transfer. In 2024 IEEE Energy Conversion Congress and Exposition (ECCE) (pp. 1887-1892). IEEE.

[18] He, Z., Qu, Y., & Jin, D. (2025, June). Real-Time Power System Event Detection on Programmable Network Switches with Synchrophasor Data. In ICC 2025-IEEE International Conference on Communications (pp. 3918-3923). IEEE.

[19] Wang, J., Feng, X., Yu, Y., Wang, X., Han, X., Shi, K., ... & Cai, J. (2024). Function-dependent neural-network-driven state feedback control and self-verification stability for discrete-time nonlinear system. Neurocomputing, 609, 128422.

[20] Zhu, G., Zhang, S., Deng, Z., Wang, J., Li, Y., Dong, J., & Bauer, P. (2025). Extended hybrid modulation for multi-stage constant-current wireless ev charging. IEEE Transactions on Power Electronics.

[21] Wang, Y., & Ling, C. (2025). Controlling attributes of. xpt files generated by R. In PharmaSUG 2025 conference proceedings. San Diego, CA.

[22] Zhu, G., Dong, J., Yu, G., Shi, W., Riekerk, C., & Bauer, P. (2024). Optimal multivariable control for wide output regulation and full-range efficiency optimization in LCC–LCC compensated wireless power transfer systems. IEEE Transactions on Power Electronics, 39(9), 11834-11848.

[23] Smith, J., Davis, E., & Inoue, S. (2026). Design Optimization of Ultra-High-Speed Photonic Devices based on InP Technology using Genetic Algorithms. Frontiers in Applied Physics and Mathematics, 3(1), 1-8.